Large $\nu_\mu \to \nu_\tau$ and $\nu_e \to \nu_\tau$ transitions in short-baseline experiments?

Carlo Giunti

INFN, Sez. di Torino, and Dip. di Fisica Teorica, Univ. di Torino, I–10125 Torino, Italy, and School of Physics, Korea Institute for Advanced Study, Seoul 130-012, Korea

Marco Laveder

Dip. di Fisica "G. Galilei", Univ. di Padova, and INFN, Sez. di Padova, I–35131 Padova, Italy
(October 13, 2000)

Abstract

Considering four-neutrino schemes of type 3+1, we identify four small regions of the neutrino mixing parameter space compatible with all data. Assuming a small mixing between the sterile neutrino and the isolated mass eigenstate we show that large $\nu_\mu \to \nu_\tau$ and $\nu_e \to \nu_\tau$ transitions are predicted in short-baseline experiments and could be observed in the near future in dedicated experiments. We discuss also implications for solar, atmospheric and long-baseline neutrino experiments and we present a formalism that allows to describe in 3+1 schemes atmospheric neutrino oscillations, long-baseline ν_μ disappearance and $\nu_\mu \to \nu_\tau$ transitions in matter.

PACS numbers: 14.60.St

Typeset using REVTEX

I. INTRODUCTION

Neutrino oscillation experiments are powerful probes of neutrino masses (see [1–6]). At present three types of neutrino oscillation experiments have obtained positive results: solar and atmospheric experiments and one short-baseline experiment.

All solar neutrino experiments (Homestake [7], Kamiokande [8], GALLEX [9], SAGE [10], Super-Kamiokande [11]) have found a deficit in the flux of electron neutrinos on Earth with respect to the Standard Solar Model prediction [12], which constitutes an indication in favor of oscillations of electron neutrinos into other states. Although no direct proof of these oscillations exist at present, there is a convincing evidence that the deficit of solar ν_e's is due to neutrino physics, of which neutrino oscillations is the simplest and most natural phenomenon. Hopefully, the issue will be definitively settled in a few years by the new generation of neutrino oscillation experiments (GNO [13], SNO [14], Borexino [15], ICARUS [16] and others [17]).

Several atmospheric neutrino experiments (Kamiokande [18], IMB [19], Super-Kamiokande [20], Soudan 2 [21], MACRO [22]) have found an anomalous ratio of the events generated by muon and electron neutrinos and an anomalous angular dependence of the events generated by muon neutrinos. Although so far the oscillation pattern has not been observed, this is considered as an evidence in favor of oscillations of muon neutrinos into tau or sterile neutrinos. Transitions of muon neutrinos into electron neutrinos are strongly disfavored by the bounds established by the long-baseline $\bar{\nu}_e$ disappearance experiments CHOOZ [23] and Palo Verde [24] and by the fact that Super-Kamiokande data do not show any anomalous angular dependence of the events generated by atmospheric electron neutrinos. The present data of the Super-Kamiokande [20] and MACRO [22] disfavor pure transitions of atmospheric muon neutrinos into sterile states. There are good chances that the issue will be clarified in a definite way in the near future by long-baseline experiments with muon neutrino beams (K2K [25], MINOS [26], OPERA [27], ICARUS [16]) and by new atmospheric neutrino experiments (MONOLITH [28] and others [29]). The K2K experiment have already obtained some preliminary indication of a possible transition of muon neutrinos into other states [30].

The third evidence in favor of neutrino oscillations has been found in the short-baseline LSND experiment [31], where an excess of e^+ events have been observed. If interpreted in terms of $\bar{\nu}_\mu \to \bar{\nu}_e$ neutrino oscillations, this excess corresponds to an oscillation probability of $(2.5 \pm 0.6 \pm 0.4) \times 10^{-3}$. This result has not been confirmed by other experiments (many other less sensitive short-baseline experiments have not found any signal of neutrino oscillations; the strongest bounds have been obtained in the Bugey [32], CDHS [33], CCFR [34], BNL-E776 [35], KARMEN [36], CHORUS [37], NOMAD [38] experiments), but it is very interesting and important, because it is the only existing evidence of neutrino flavor transition from one state to another and because such transitions could be explored with high accuracy in future short-baseline experiments. In a few years the MiniBooNE experiment [39] will check the LSND signal in terms of neutrino oscillations.

It is well known (see [40,41]) that the three indications in favor of neutrino oscillations need at least three different neutrino mass-squared differences (Δm^2's), arranged in the hierarchical order $\Delta m^2_{\mathrm{SUN}} \ll \Delta m^2_{\mathrm{ATM}} \ll \Delta m^2_{\mathrm{SBL}}$. This means that at least four massive neutrinos must exist. Here we consider the minimal case of four massive neutrinos, that

has been considered recently by many authors (see [42–52,6,40] and references therein), whose flavor basis is constituted by the standard active neutrinos ν_e, ν_μ, ν_τ, and a sterile neutrino ν_s. Figure 1 shows the six possible four-neutrino schemes that can accommodate the observed hierarchy of Δm^2's. These six schemes are divided in two classes: 3+1 and 2+2. In the 3+1 schemes there is a group of three neutrino masses separated from an isolated mass by the LSND gap of the order of 1 eV, such that the largest mass-squared difference, Δm_{41}^2 (where $\Delta m_{kj}^2 \equiv m_k^2 - m_j^2$ and m_k, m_j are neutrino masses, with $k, j = 1, \ldots, 4$), generates the oscillations observed in the LSND experiment. In the 2+2 schemes there are two couples of close mass eigenstates separated by the LSND gap. The numbering of the mass eigenvalues in Fig. 1 is conveniently chosen in order to have always solar neutrino oscillations generated by $\Delta m_{21}^2 = \Delta m_{\text{SUN}}^2$ and short-baseline (SBL) oscillations generated by $|\Delta m_{41}^2| \simeq |\Delta m_{42}^2| = \Delta m_{\text{SBL}}^2$ (we have also $|\Delta m_{41}^2| \simeq |\Delta m_{43}^2|$ in 3+1 schemes and $|\Delta m_{41}^2| \simeq |\Delta m_{31}^2| \simeq |\Delta m_{32}^2|$ in 2+2 schemes). In 3+1 schemes atmospheric neutrino oscillations are generated by $|\Delta m_{31}^2| \simeq |\Delta m_{32}^2| = \Delta m_{\text{ATM}}^2$, whereas in 2+2 schemes they are generated by $|\Delta m_{43}^2| = \Delta m_{\text{ATM}}^2$.

It has been shown that in the framework of four-neutrino mixing the 3+1 schemes are disfavored by the experimental data, with respect to the 2+2 schemes [42–44,40]. However, in a recent paper Barger, Kayser, Learned, Weiler and Whisnant [52] noticed that the new 99% CL allowed region obtained recently in the LSND experiment and presented at the Neutrino 2000 conference allows the existence 3+1 schemes (see also [49]) in four small regions of the amplitude $A_{\mu e}$ of $\nu_\mu \to \nu_e$ and $\bar\nu_\mu \to \bar\nu_e$ oscillations ($A_{\mu e}$ is equivalent to the usual $\sin^2 2\vartheta$ in the two-generation case). These regions, to be derived later (Eqs. (3.1)–(3.6)) are shown in Fig. 2, enclosed by very thick solid lines. They lay at

$$\text{R1:} \quad |\Delta m_{41}^2| \simeq 0.25 \, \text{eV}^2 \,,$$
$$\text{R2:} \quad |\Delta m_{41}^2| \simeq 0.9 \, \text{eV}^2 \,,$$
$$\text{R3:} \quad |\Delta m_{41}^2| \simeq 1.7 \, \text{eV}^2 \,,$$
$$\text{R4:} \quad |\Delta m_{41}^2| \simeq 6 \, \text{eV}^2 \,. \tag{1.1}$$

Barger, Kayser, Learned, Weiler and Whisnant explored the phenomenological consequences of the assumption

$$1 - |U_{s4}|^2 \ll 1 \tag{1.2}$$

(here $U_{\alpha k}$ are the elements of the 4×4 neutrino mixing matrix with $\alpha = s, e, \mu, \tau$ and $k = 1, \ldots, 4$). Such a scheme is attractive because it represents a perturbation of the standard three-neutrino mixing in which a mass eigenstate is added, that mixes mainly with the new sterile neutrino ν_s and very weakly with the standard active neutrinos ν_e, ν_μ and ν_τ. In this case, the usual phenomenology of three-neutrino mixing in solar and atmospheric neutrino oscillation experiments is practically unchanged. The atmospheric neutrino anomaly would be explained by dominant $\nu_\mu \to \nu_\tau$ transitions, with possible subdominant $\nu_\mu \leftrightarrows \nu_e$ transitions constrained by the CHOOZ bound [53,54,50]. The solar neutrino problem would be explained by an approximately equal mixture of $\nu_e \to \nu_\mu$ and $\nu_e \to \nu_\tau$ transitions [54,55].

Here, we consider another possibility that, as we will see, predicts relative large $\nu_\mu \to \nu_\tau$ and $\nu_e \to \nu_\tau$ transitions in short-baseline neutrino oscillation experiments, that could be observed in the near future. We consider the 3+1 schemes with

$$|U_{s4}|^2 \ll 1 \,. \tag{1.3}$$

This could be obtained, for example, in the hierarchical scheme I (see Fig. 1) with an appropriate symmetry keeping the sterile neutrino very light, *i.e.* mostly mixed with the lightest mass eigenstates. Notice that nothing forbids $|U_{s4}|^2$ to be even zero exactly.

II. 3+1 SCHEMES WITH $|U_{s4}|^2 \ll 1$

From the assumption (1.3), since the amplitude of $\nu_\alpha \to \nu_\beta$ and $\nu_\beta \to \nu_\alpha$ oscillations in short-baseline neutrino oscillation experiments (equivalent to the usual $\sin^2 2\vartheta$ in the two-generation case) is given by [42,6]

$$A_{\alpha\beta} = A_{\beta\alpha} = 4|U_{\alpha 4}|^2 |U_{\beta 4}|^2 \qquad (\alpha, \beta = s, e, \mu, \tau) \,, \tag{2.1}$$

we have

$$A_{\alpha s} \ll 1 \qquad (\alpha = e, \mu, \tau) \,, \tag{2.2}$$

i.e. the transitions from active to sterile neutrinos in short-baseline experiments are strongly suppressed. In the following we will neglect them.

Let us consider now the oscillation amplitude (equivalent to the usual two-generation $\sin^2 2\vartheta$) in short-baseline ν_α disappearance experiments, which is given by [42,6]

$$B_\alpha = |U_{\alpha 4}|^2 \left(1 - |U_{\alpha 4}|^2\right) \,. \tag{2.3}$$

In general the oscillation amplitude in ν_α disappearance experiments is related to the amplitude of $\nu_\alpha \to \nu_\beta$ oscillations by the relation

$$B_\alpha = \sum_{\beta \neq \alpha} A_{\alpha\beta} \,, \tag{2.4}$$

that quantify the conservation of probability. Using Eq. (2.2), Eq. (2.4) gives

$$A_{e\tau} \simeq B_e - A_{\mu e} \,. \tag{2.5}$$
$$A_{\mu\tau} \simeq B_\mu - A_{\mu e} \,. \tag{2.6}$$

Therefore, we have

$$B_e^{\min} - A_{\mu e}^{\max} \lesssim A_{e\tau} \lesssim B_e^{\max} - A_{\mu e}^{\min} \,. \tag{2.7}$$
$$B_\mu^{\min} - A_{\mu e}^{\max} \lesssim A_{\mu\tau} \lesssim B_\mu^{\max} - A_{\mu e}^{\min} \,. \tag{2.8}$$

Let us determine $B_e^{\min}$, $B_e^{\max}$, $B_\mu^{\min}$, $B_\mu^{\max}$, $A_{\mu e}^{\min}$, $A_{\mu e}^{\max}$ from the results of short-baseline experiments.

4

III. GENERAL BOUNDS IN 3+1 SCHEMES AND $\nu_\mu \to \nu_e$ SHORT-BASELINE TRANSITIONS

The values of $B_e^{\max}$ and $B_\mu^{\max}$ are given by the exclusion plots of $\bar{\nu}_e$ and ν_μ disappearance experiments (notice that $B_e^{\max}$ and $B_\mu^{\max}$ depend on $|\Delta m_{41}^2|$). The most stringent bounds for $|\Delta m_{41}^2|$ in the LSND-allowed region are given by the exclusion curves of the Bugey [32] and CHOOZ [23] reactor $\bar{\nu}_e$ disappearance experiments and the exclusion curve of the CDHS accelerator ν_μ disappearance experiment [33].

The bounds $B_e \leq B_e^{\max}$ and $B_\mu \leq B_\mu^{\max}$, together with the results of solar and atmospheric neutrino experiments imply that $|U_{e4}|^2$ and $|U_{\mu4}|^2$ are small [42,44,40]:

$$|U_{e4}|^2 \leq |U_{e4}|_{\max}^2 \quad \text{and} \quad |U_{\mu4}|^2 \leq |U_{\mu4}|_{\max}^2 \,, \tag{3.1}$$

where $|U_{e4}|_{\max}^2$ and $|U_{\mu4}|_{\max}^2$ are given by

$$|U_{e4}|_{\max}^2 = \frac{1}{2}\left(1 - \sqrt{1 - B_e^{\max}}\right) \,, \tag{3.2}$$

$$|U_{\mu4}|_{\max}^2 = \min\left[\frac{1}{2}\left(1 - \sqrt{1 - B_\mu^{\max}}\right) , 0.55\right] \,. \tag{3.3}$$

The number 0.55 comes [44] from the up-down asymmetry of multi-GeV muon-like events measured in the Super-Kamiokande experiment [20]. The values of $|U_{e4}|_{\max}^2$ and $|U_{\mu4}|_{\max}^2$ as functions of $|\Delta m_{41}^2|$ are shown, respectively, in Figs. 3 and 4.

In the 3+1 schemes we have

$$A_{\mu e} = 4|U_{\mu4}|^2|U_{e4}|^2 \,, \tag{3.4}$$

and the bounds (3.1) imply that [42]

$$A_{\mu e} \leq 4|U_{\mu4}|_{\max}^2|U_{e4}|_{\max}^2 \,. \tag{3.5}$$

As one can see from Fig. 2, from the LSND region constrained by the exclusion curves of KARMEN and BNL-E776 and by the bound (3.5), there are four allowed regions for $A_{\mu e}$, R1, R2, R3, R4 in Eq. (1.1), where we have

$$A_{\mu e}^{\min} \leq 4|U_{\mu4}|^2|U_{e4}|^2 \leq A_{\mu e}^{\max} \,. \tag{3.6}$$

These regions could be explored in the near future by the MiniBooNE experiment [39]. Region R4 is at the limit of the final NOMAD sensitivity in the $\nu_\mu \to \nu_e$ channel [56].

From the lower bound in Eq. (3.6) and the bounds (3.1), we obtain

$$|U_{e4}|^2 \geq \frac{A_{\mu e}^{\min}}{4|U_{\mu4}|^2} \geq \frac{A_{\mu e}^{\min}}{4|U_{\mu4}|_{\max}^2} \,, \tag{3.7}$$

$$|U_{\mu4}|^2 \geq \frac{A_{\mu e}^{\min}}{4|U_{e4}|^2} \geq \frac{A_{\mu e}^{\min}}{4|U_{e4}|_{\max}^2} \,. \tag{3.8}$$

Therefore, we have

$$\frac{A_{\mu e}^{\min}}{4|U_{\mu 4}|_{\max}^2} \leq |U_{e4}|^2 \leq |U_{e4}|_{\max}^2 \,, \tag{3.9}$$

$$\frac{A_{\mu e}^{\min}}{4|U_{e4}|_{\max}^2} \leq |U_{\mu 4}|^2 \leq |U_{\mu 4}|_{\max}^2 \,. \tag{3.10}$$

Since these bounds have been obtained without any assumption on the value of $|U_{s4}|^2$, they are generally valid in any 3+1 scheme. The corresponding four allowed regions for $|U_{e4}|^2$ and $|U_{\mu 4}|^2$ are shown, respectively, in Figs. 3 and 4.

The lower bounds for $|U_{e4}|^2$ and $|U_{\mu 4}|^2$ in Eqs. (3.7) and (3.8) imply lower bounds for the oscillation amplitudes $B_e = 4|U_{e4}|^2 \left(1 - |U_{e4}|^2\right)$ and $B_\mu = 4|U_{\mu 4}|^2 \left(1 - |U_{\mu 4}|^2\right)$. Let us derive these bounds.

Since $|U_{e4}|_{\max}^2$ is always smaller than $1/2$, the lower bound for B_e is

$$B_e^{\min} = \frac{A_{\mu e}^{\min}}{|U_{\mu 4}|_{\max}^2} \left(1 - \frac{A_{\mu e}^{\min}}{4|U_{\mu 4}|_{\max}^2}\right) \,. \tag{3.11}$$

On the other hand, since $|U_{\mu 4}|_{\max}^2$ can be bigger than $1/2$, the lower bound for B_μ is

$$B_\mu^{\min} = \min\left[\frac{A_{\mu e}^{\min}}{|U_{e4}|_{\max}^2} \left(1 - \frac{A_{\mu e}^{\min}}{4|U_{e4}|_{\max}^2}\right) \,,\, |U_{\mu 4}|_{\max}^2 \left(1 - |U_{\mu 4}|_{\max}^2\right)\right] \,. \tag{3.12}$$

Figure 5 and 6 show the allowed regions in the B_e–$|\Delta m_{41}^2|$ and B_μ–$|\Delta m_{41}^2|$ planes given by the bounds

$$B_\alpha^{\min} \leq B_\alpha \leq B_\alpha^{\max} \qquad (\alpha = e, \mu) \,. \tag{3.13}$$

One can see that these regions lie just on the left of the Bugey+CHOOZ (Fig. 5) and CDHS (Fig. 6) exclusion curves and could be observed in the near future [57]. Let us emphasize that these regions are generally predicted in any 3+1 scheme, since they have been obtained independently on any assumption on the mixing (as Eq. (1.2) or Eq. (1.3)).

IV. LARGE $\nu_e \to \nu_\tau$ AND $\nu_\mu \to \nu_\tau$ SHORT-BASELINE TRANSITIONS

We have now all the elements to calculate the bounds (2.7) and (2.8) on the amplitudes of short-baseline $\nu_e \to \nu_\tau$ and $\nu_\mu \to \nu_\tau$ oscillations that follow from the assumption (1.3), $|U_{s4}|^2 \ll 1$.

Figure 7 shows the allowed regions in the $A_{\mu\tau}$–$|\Delta m_{41}^2|$ plane given by the bounds (2.8). One can see that the region R4 is excluded by the negative results of the CHORUS [37] and NOMAD [38] experiments. The other three regions are possible and predict relatively large oscillation amplitudes that could be observed in the near future, especially the two regions R2 and R3 in which $A_{\mu\tau} \sim 4 \times 10^{-2} - 10^{-1}$.

Figure 8 shows the allowed regions in the $A_{e\tau}$–$|\Delta m_{41}^2|$ plane given by the bounds (2.7). One can see that these regions predict relatively large oscillation amplitudes, but unfortunately lie rather far from the CHORUS and NOMAD exclusion curves (except the region R4 that is excluded by Fig. 7). Therefore, even under the favorable assumption (1.3), it will be

very difficult to observe $\nu_e \to \nu_\tau$ transitions in short baseline experiments with conventional neutrino beams, but large transitions could be observed with a ν_e beam from a neutrino factory [58].

As one can see from Fig. 3, the bound in Eq. (3.1) imply that $|U_{e4}|^2$ is very small in all the three allowed regions in Fig. 7. On the other hand, one can see from Fig. 4 that $|U_{\mu4}|^2$ is small in the two allowed regions R2 and R3, but it is large in the region R1. As a consequence of the unitarity of the mixing matrix and the assumption (1.3), we have $1 - |U_{\tau4}|^2 \ll 1$ in R2 and R3, whereas $|U_{\tau4}|^2$ can be as small as about $1/2$ in R1. The prediction for solar, atmospheric and long-baseline experiments depend on the value of $|U_{\mu4}|^2$. There are two possibilities:

1. $|U_{\mu4}|^2 \ll 1$ in regions R2 and R3 in Fig. 4. In this case $1 - |U_{\tau4}|^2 \ll 1$ and the atmospheric neutrino anomaly is due to dominant $\nu_\mu \to \nu_s$ transitions. This possibility is disfavored by present Super-Kamiokande and MACRO data [20,22], but still it is not completely excluded (see [59,60,51]). Obviously, in this case long-baseline $\nu_\mu \to \nu_\tau$ transitions are suppressed with respect to the dominant $\nu_\mu \to \nu_s$ transitions, that are almost entirely responsible of the disappearance of ν_μ's.

   The solar neutrino problem is due to an approximately equal mixture of $\nu_e \to \nu_\mu$ and $\nu_e \to \nu_s$ transitions, which is allowed by the data. This has been shown in Refs. [46,47] in the framework of the 2+2 schemes in Fig. 1. However, the results obtained in Refs. [46,47] are valid also in the 3+1 schemes, because the formalism of solar neutrino oscillations in 3+1 schemes is identical to that in 2+2 schemes [45–47]. Indeed, from Eqs. (3.1) and (3.2) we already know that the results of the Bugey and CHOOZ experiment imply that $|U_{e4}|^2$ is very small. Furthermore, taking into account the hierarchy

   $$\Delta m_{21}^2 = \Delta m_{\mathrm{SUN}}^2 \ll |\Delta m_{31}^2| = \Delta m_{\mathrm{ATM}}^2 \ll |\Delta m_{41}^2| = \Delta m_{\mathrm{SBL}}^2 , \qquad (4.1)$$

   the effective survival probability of $\bar{\nu}_e$ and ν_e in long-baseline experiments is given by

   $$P_{\nu_e \to \nu_e}^{\mathrm{LBL}} = 1 - 4|U_{e3}|^2 \left(1 - |U_{e3}|^2\right) \sin^2\left(\frac{\Delta m_{31}^2 L}{4E}\right) + |U_{e4}|^4 , \qquad (4.2)$$

   where L is the propagation distance and E is the neutrino energy. Neglecting $|U_{e4}|^4$, Eq. (4.2) has the same structure as the usual two-generation survival probability (see [6]), with $\sin^2 2\vartheta$ replaced by $4|U_{e3}|^2 \left(1 - |U_{e3}|^2\right)$ and Δm^2 replaced by Δm_{31}^2. The bound on $\sin^2 2\vartheta$ obtained in the CHOOZ experiment [23] for $|\Delta m_{31}^2| \gtrsim 10^{-3}\,\mathrm{eV}^2$ implies that $|U_{e3}|^2 \lesssim 2.6 \times 10^{-2}$. Therefore, both $|U_{e3}|^2$ and $|U_{e4}|^2$ are very small,

   $$|U_{e3}|^2 \lesssim 3 \times 10^{-2} \qquad |U_{e4}|^2 \lesssim 3 \times 10^{-2} , \qquad (4.3)$$

   and can be neglected in the study of solar neutrino oscillations, as done in Refs. [45–47]. In other words, the production and detection of the mass eigenstates ν_3 and ν_4 is negligibly small in solar neutrino experiments. Moreover, because of the hierarchy (4.1), there are no matter-induced transitions from ν_1, ν_2 to ν_3, ν_4. Hence, ν_3 and ν_4 effectively decouple in solar neutrino oscillations, leading to the formalism described in Refs. [45–47].

2. $|U_{\mu 4}|^2 \simeq 0.33 - 0.55$ in region R1 in Fig. 4. In this case the solar neutrino problem is due to a mixture of $\nu_e \to \nu_\mu$, $\nu_e \to \nu_\tau$ and $\nu_e \to \nu_s$ transitions, that is allowed by data as in the previous case.

   The atmospheric neutrino anomaly is due a mixture of $\nu_\mu \to \nu_\tau$ and $\nu_\mu \to \nu_s$ transitions. In Refs. [48,50,51] it has been shown that a mixture of $\nu_\mu \to \nu_\tau$ and $\nu_\mu \to \nu_s$ transitions in the framework of 2+2 schemes is allowed by the atmospheric neutrino data. This indicates that such a mixture should be allowed also in the framework of 3+1 schemes. The groups specialized in the analysis of atmospheric neutrino data could check this possibility using the formalism presented in Appendix A. The existence of mixed $\nu_\mu \to \nu_\tau$ and $\nu_\mu \to \nu_s$ transitions can also be checked by comparing the rates of ν_μ disappearance and $\nu_\mu \to \nu_\tau$ appearance in future long-baseline experiments with ν_μ beams. The formalism that allows to describe these oscillation channels in the framework of 3+1 four-neutrino schemes is presented in Appendix A.

These predictions are testable in future experiments, especially measuring the percentage of transitions into active and sterile neutrinos in solar, atmospheric and long-baseline experiments (that should measure the same transitions observed in atmospheric neutrino experiments). Taking into account also the prediction of large $\nu_\mu \to \nu_\tau$ and $\nu_e \to \nu_\tau$ in short-baseline experiments, the schemes under consideration can be checked and possibly falsified in the near future.

V. CONCLUSIONS

In conclusion, we have considered the four-neutrino 3+1 schemes in Fig. 1, that are marginally allowed by present data (see Fig. 2). We have identified four small regions in the parameter space of neutrino mixing compatible with all data and we have derived general upper and lower bounds for the elements U_{e4} and $U_{\mu 4}$ of the mixing matrix and on the oscillation amplitudes in short-baseline $\bar\nu_e$ and ν_μ disappearance experiments. The corresponding $\nu_\mu \to \nu_e$ transitions and ν_e and ν_μ disappearance in short-baseline experiments are relatively large and could be observed in future dedicated experiments. Assuming a small mixing of the sterile neutrino with the isolated mass eigenstate, $|U_{s4}|^2 \ll 1$, we have shown that large $\nu_\mu \to \nu_\tau$ and $\nu_e \to \nu_\tau$ transitions are predicted in short-baseline experiments. We have also discussed the implications of $|U_{s4}|^2 \ll 1$ for solar, atmospheric and long-baseline neutrino oscillation experiments and we have presented in Appendix A the formalism describing in general 3+1 schemes the oscillations in matter of atmospheric neutrinos and neutrinos in long-baseline ν_μ disappearance and $\nu_\mu \to \nu_\tau$ appearance experiments. Finally, let us remark that the four 3+1 schemes in Fig. 1 are equivalent for solar, atmospheric and short-baseline neutrino oscillation experiments, but they may be distinguishable in long-baseline $\nu_\mu \to \nu_e$ experiments if $|U_{e3}|^2$ is not too small [61], or through their different effects in tritium β decay and neutrinoless double-β decay (see [3,5,6]) and through neutrino oscillations in supernovae (see [62,63]) and in the early universe (see [64–68]).

ACKNOWLEDGMENTS

APPENDIX A: FORMALISM OF ATMOSPHERIC NEUTRINO OSCILLATIONS

In this appendix we derive in a concise way the formalism in 3+1 schemes of atmospheric neutrino oscillations and oscillations in long-baseline $\nu_\mu \to \nu_\tau$ and ν_μ disappearance experiments. We take into account matter effects, following a method similar to that used in Ref. [45] in the case of 2+2 schemes. As explained in the main text, the formalism of solar neutrino oscillations in 3+1 schemes is identical to that in 2+2 schemes [45–47].

From Eq. (4.3) we know that U_{e3} and U_{e4} can be neglected. Choosing the ordering ν_s, ν_e, ν_μ, ν_τ for the flavor neutrino fields, the mixing matrix can be written as

$$U = V_{34} V_{14} V_{13} V_{12} , \tag{A1}$$

where

$$(V_{ij})_{ab} = \delta_{ab} + (\cos\vartheta_{ij} - 1)(\delta_{ia}\delta_{ib} + \delta_{ja}\delta_{jb}) + \sin\vartheta_{ij}(\delta_{ia}\delta_{jb} - \delta_{ja}\delta_{ib}) \tag{A2}$$

represents a rotation by an angle ϑ_{ij} in the i-j plane. We have also neglected possible CP-violating phases. The evolution of the neutrino flavor amplitudes ψ_α ($\alpha = s, e, \mu, \tau$) in vacuum and in matter is given by the MSW equation [69]

$$i \frac{\mathrm{d}}{\mathrm{d}x} \Psi = \mathcal{H} \Psi , \tag{A3}$$

where $\Psi = (\psi_s, \psi_e, \psi_\mu, \psi_\tau)^T$ and $\mathcal{H}$ is the effective Hamiltonian

$$\mathcal{H} = \frac{1}{2p} \left(U \mathcal{M}_0^2 U^\dagger + \mathcal{A} \right) . \tag{A4}$$

Here p is the neutrino momentum,

$$\mathcal{M}_0^2 = \mathrm{diag}(0, 0, \Delta m_{31}^2, \Delta m_{41}^2) \tag{A5}$$

is the mass-squared matrix, in which we neglected Δm_{21}^2 according to the hierarchical relation (4.1), and $\mathcal{A}$ is the matrix

$$\mathcal{A} = \mathrm{diag}(-A_{NC}, A_{CC}, 0, 0) , \tag{A6}$$

with $A_{CC} = 2pV_{CC}$ and $A_{NC} = 2pV_{NC}$, where V_{CC} and V_{NC} are, respectively, the matter-induced charged-current and neutral-current potentials (see [2–6]). For atmospheric neutrinos propagating in the Earth and accelerator neutrinos in long-baseline experiments $|A_{CC}| \sim |A_{NC}| \sim |\Delta m_{31}^2| \ll |\Delta m_{41}^2|$. In Eq. (A4) we have neglected a common phase for the flavor amplitudes, that is irrelevant for neutrino oscillations.

The evolution equation (A3) is most easily solved in the rotated basis $\Psi' = V_{14}^T V_{34}^T \Psi = (\psi_1', \psi_2', \psi_3', \psi_4')^T$ that obeys to a similar evolution equation, with $\mathcal{H}$ replaced by

$$\mathcal{H}' = \frac{1}{2p} \left(V_{13} \mathcal{M}_0^2 V_{13}^T + V_{14}^T \mathcal{A} V_{14} \right) \tag{A7}$$

where we have taken into account the fact that $V_{12}\mathcal{M}_0^2 V_{12}^T = \mathcal{M}_0^2$ and $V_{34}^T \mathcal{A} V_{34} = \mathcal{A}$, which lead to a significant simplification of the evolution equation. The explicit form of $\mathcal{H}'$ is

$$
\mathcal{H}' = \frac{1}{4p} \begin{pmatrix} (1-c_{2\vartheta_{13}})\Delta m_{31}^2 - 2c_{\vartheta_{14}}^2 A_{NC} & 0 & s_{2\vartheta_{13}}\Delta m_{31}^2 & -s_{2\vartheta_{14}} A_{NC} \\ 0 & 2A_{CC} & 0 & 0 \\ s_{2\vartheta_{13}}\Delta m_{31}^2 & 0 & (1+c_{2\vartheta_{13}})\Delta m_{31}^2 & 0 \\ -s_{2\vartheta_{14}} A_{NC} & 0 & 0 & 2\Delta m_{41}^2 - 2s_{\vartheta_{14}}^2 A_{NC} \end{pmatrix}, \tag{A8}
$$

with $c_\vartheta \equiv \cos\vartheta$ and $s_\vartheta \equiv \sin\vartheta$. This equation shows that the amplitudes ψ_2' and ψ_4' evolve independently (remember that $|\Delta m_{41}^2| \gg |A_{NC}|$), with phases given by the energy eigenvalues

$$
E_2' = A_{CC}/2p = V_{CC}, \quad E_4' \simeq \Delta m_{41}^2/2p, \tag{A9}
$$

whereas the evolutions of the amplitudes ψ_1' and ψ_3' are coupled and there is a resonance in the 1-3 sector for

$$
-\cos^2 \vartheta_{14} A_{NC} = \cos 2\vartheta_{13} \Delta m_{31}^2. \tag{A10}
$$

Notice that for neutrinos the left-hand side of Eq. (A10) is positive, because $A_{NC} \leq 0$, whereas for antineutrinos it is negative because A_{NC} must be replaced by $\overline{A}_{NC} = -A_{NC}$. Hence, if $\Delta m_{31}^2 > 0$ (schemes I and IV in Fig. 1) and $\vartheta_{13} < \pi/4$ or $\Delta m_{31}^2 < 0$ (schemes II and III) and $\vartheta_{13} > \pi/4$, there can be a resonance for neutrinos, otherwise the resonance can be for antineutrinos.

One can calculate the evolution of the amplitudes ψ_1' and ψ_3' solving numerically the two coupled equations generated by the 1-3 sector of the effective Hamiltonian $\mathcal{H}'$. Another common method for the solution of the evolution equation is to divide the Earth interior into shell with constant density, calculate the evolution of the amplitudes Ψ' in each shell and match the amplitudes in the flavor basis at the shell boundaries. In this case, in each shell the amplitudes ψ_1' and ψ_3' can be written as

$$
\psi_1' = \cos\vartheta_{13}^M \psi_1^M + \sin\vartheta_{13}^M \psi_3^M, \quad \psi_3' = -\sin\vartheta_{13}^M \psi_1^M + \cos\vartheta_{13}^M \psi_3^M, \tag{A11}
$$

where ψ_1^M and ψ_3^M are the amplitudes of the energy eigenstates that evolve with phases given by the energy eigenvalues

$$
E_{1,3}^M = \frac{1}{4p} \left[\Delta m_{31}^2 - \cos^2 \vartheta_{14} A_{NC} \mp \sqrt{(\cos 2\vartheta_{13}\Delta m_{31}^2 + \cos^2 \vartheta_{14} A_{NC})^2 + (\sin 2\vartheta_{13}\Delta m_{31}^2)^2} \right]. \tag{A12}
$$

The effective mixing angle in matter ϑ_{13}^M is given by

$$
\tan 2\vartheta_{13}^M = \frac{\sin 2\vartheta_{13}\Delta m_{31}^2}{\cos 2\vartheta_{13}\Delta m_{31}^2 + \cos^2 \vartheta_{14} A_{NC}}, \tag{A13}
$$

from which one can see that $\vartheta_{13}^M = \pi/4$ when the resonance condition (A10) is satisfied, and $\vartheta_{13}^M \to \pi/2$ in a very dense medium, where $|\cos^2 \vartheta_{14} A_{NC}| \gg |\cos 2\vartheta_{13}\Delta m_{31}^2|$ if $\cos 2\vartheta_{13}\Delta m_{31}^2 > 0$, whereas $\vartheta_{13}^M \to 0$ in a very dense medium if $\cos 2\vartheta_{13}\Delta m_{31}^2 < 0$.

The connection between the amplitudes Ψ' and the flavor amplitudes Ψ, needed for the calculation of the probability of flavor transitions, is given by

$$
\begin{aligned}
\psi_s &= \cos\vartheta_{14}\psi_1' + \sin\vartheta_{14}\psi_4'\,, \\
\psi_e &= \psi_2'\,, \\
\psi_\mu &= -\sin\vartheta_{14}\sin\vartheta_{34}\psi_1' + \cos\vartheta_{34}\psi_3' + \cos\vartheta_{14}\sin\vartheta_{34}\psi_4'\,, \\
\psi_\tau &= -\sin\vartheta_{14}\cos\vartheta_{34}\psi_1' - \sin\vartheta_{34}\psi_3' + \cos\vartheta_{14}\cos\vartheta_{34}\psi_4'\,.
\end{aligned}
\tag{A14}
$$

The second line of Eq. (A14) imply that electron neutrinos do not oscillate in atmospheric neutrino experiments (remember that ψ_2' evolves independently). This is due to the approximation $U_{e3} = 0$, motivated by Eq. (4.3), which also imply that the charged-current matter potential V_{CC}, felt only by ν_e, is irrelevant for atmospheric neutrino oscillations (only the neutral-current potential V_{NC}, felt by ν_μ and ν_τ, enter in Eqs. (A10)–(A13)). On the other hand, simultaneous $\nu_\mu \to \nu_\tau$ and $\nu_\mu \to \nu_s$ transitions are allowed, with pure $\nu_\mu \to \nu_\tau$ transitions in the limit $\cos\vartheta_{14} = 0$, that corresponds to $U_{s4} = 1$, and pure $\nu_\mu \to \nu_s$ transitions in the limit $\cos\vartheta_{14}\cos\vartheta_{34} = 1$, that corresponds to $U_{\tau 4} = 1$.

Let us consider finally long baseline experiments in which the neutrino beam travels in the crust of the Earth, where the matter density is practically constant. The probability of $\nu_\alpha \to \nu_\beta$ transitions is given by

$$
\begin{aligned}
P^{\mathrm{LBL}}_{\nu_\alpha \to \nu_\beta} &= \left| U^M_{\alpha 1}U^M_{\beta 1} + U^M_{\alpha 3}U^M_{\beta 3}\exp\left(-i\frac{\Delta^M_{31}L}{2p}\right)\right|^2 + |U^M_{\alpha 4}|^2|U^M_{\beta 4}|^2 \\
&= -4U^M_{\alpha 1}U^M_{\beta 1}U^M_{\alpha 3}U^M_{\beta 3}\sin^2\left(\frac{\Delta^M_{31}L}{4p}\right) + 2|U^M_{\alpha 4}|^2|U^M_{\beta 4}|^2\,,
\end{aligned}
\tag{A15}
$$

where L is the propagation distance,

$$
\Delta^M_{31} = 2p\left(E^M_3 - E^M_1\right) = \sqrt{\left(\cos 2\vartheta_{13}\Delta m^2_{31} + \cos^2\vartheta_{14}\,A_{NC}\right)^2 + \left(\sin 2\vartheta_{13}\Delta m^2_{31}\right)^2}\,,
\tag{A16}
$$

and U^M is the effective mixing matrix in matter,

$$
U^M = V_{34}V_{14}V^M_{13} = \begin{pmatrix}
c_{\vartheta_{14}}c_{\vartheta^M_{13}} & 0 & c_{\vartheta_{14}}s_{\vartheta^M_{13}} & s_{\vartheta_{14}} \\
0 & 1 & 0 & 0 \\
-s_{\vartheta_{34}}s_{\vartheta_{14}}c_{\vartheta^M_{13}}-c_{\vartheta_{34}}s_{\vartheta^M_{13}} & 0 & -s_{\vartheta_{34}}s_{\vartheta_{14}}s_{\vartheta^M_{13}}+c_{\vartheta_{34}}c_{\vartheta^M_{13}} & s_{\vartheta_{34}}c_{\vartheta_{14}} \\
-c_{\vartheta_{34}}s_{\vartheta_{14}}c_{\vartheta^M_{13}}+s_{\vartheta_{34}}s_{\vartheta^M_{13}} & 0 & -c_{\vartheta_{34}}s_{\vartheta_{14}}s_{\vartheta^M_{13}}-s_{\vartheta_{34}}c_{\vartheta^M_{13}} & c_{\vartheta_{34}}c_{\vartheta_{14}}
\end{pmatrix}\,,
\tag{A17}
$$

where V^M_{13} is equal to V_{13} with ϑ_{13} replaced by ϑ^M_{13}. The expression (A15) can be used to analyze the data of long-baseline $\nu_\mu \to \nu_\tau$ and ν_μ disappearance experiments (the analysis of long-baseline $\nu_\mu \to \nu_e$ data requires the relaxation of the approximation $U_{e3} = 0$, leading to a significant complication of the formalism [61]).

REFERENCES

[1] S. M. Bilenky and B. Pontecorvo, Phys. Rept. **41**, 225 (1978).

[2] S. P. Mikheev and A. Y. Smirnov, Sov. Phys. Usp. **30**, 759 (1987).

[3] S. M. Bilenky and S. T. Petcov, Rev. Mod. Phys. **59**, 671 (1987).

[4] T. K. Kuo and J. Pantaleone, Rev. Mod. Phys. **61**, 937 (1989).

[5] C. W. Kim and A. Pevsner, *Neutrinos in physics and astrophysics* (Harwood Academic Press, Chur, Switzerland, 1993), Contemporary Concepts in Physics, Vol. 8.

[6] S. M. Bilenky, C. Giunti, and W. Grimus, Prog. Part. Nucl. Phys. **43**, 1 (1999), hep-ph/9812360.

[7] B. T. Cleveland *et al.*, Astrophys. J. **496**, 505 (1998).

[8] Kamiokande, Y. Fukuda *et al.*, Phys. Rev. Lett. **77**, 1683 (1996).

[9] GALLEX, W. Hampel *et al.*, Phys. Lett. **B447**, 127 (1999).

[10] SAGE, J. N. Abdurashitov *et al.*, Phys. Rev. **C60**, 055801 (1999), astro-ph/9907113.

[11] Y. Suzuki (Super-Kamiokande Coll.), Talk presented at Neutrino 2000, Sudbury, Canada, 16–21 June 2000 (http://nu2000.sno.laurentian.ca); Talk presented at NOW2000, Otranto, Italy, September 2000 (http://www.ba.infn.it/~now2000).

[12] J. N. Bahcall, S. Basu, and M. H. Pinsonneault, Phys. Lett. **B433**, 1 (1998), astro-ph/9805135.

[13] GNO, M. Altmann *et al.*, (2000), hep-ex/0006034.

[14] SNO, A. Hallin, Nucl. Phys. **A663-664**, 787 (2000).

[15] Borexino, A. Ianni, Nucl. Phys. **A663-664**, 791 (2000).

[16] C. Vignoli *et al.* (ICARUS Coll.), Nucl. Phys. Proc. Suppl. **85**, 119 (2000); P. Cennini *et al.* (ICARUS Coll.), LNGS-94/99-I (1994); Web page: http://pcnometh4.cern.ch.

[17] F. von Feilitzsch, Talk presented at Neutrino 2000, Sudbury, Canada, 16–21 June 2000 (http://nu2000.sno.laurentian.ca);.

[18] Y. Fukuda *et al.* (Kamiokande Coll.), Phys. Lett. B **335**, 237 (1994).

[19] R. Becker-Szendy *et al.* (IMB Coll.), Nucl. Phys. B (Proc. Suppl.) **38**, 331 (1995).

[20] S. Fukuda *et al.* (Super-Kamiokande Coll.), hep-ex/0009001; T. Kajita (Super-Kamiokande Coll.), Talk presented at NOW2000, Otranto, Italy, September 2000 (http://www.ba.infn.it/~now2000).

[21] W.W.M. Allison *et al.* (Soudan 2 Coll.), Phys. Lett. B **449**, 137 (1999).

[22] F. Ronga (Macro Coll.), Talk presented at NOW2000, Otranto, Italy, September 2000 (http://www.ba.infn.it/~now2000).

[23] M. Apollonio *et al.* (CHOOZ Coll.), Phys. Lett. B **420**, 397 (1998), hep-ex/9711002; Phys. Lett. B **466**, 415 (1999), hep-ex/9907037.

[24] F. Boehm *et al.* (Palo Verde Coll.), hep-ex/0003022.

[25] Y. Oyama (K2K Coll.), hep-ex/9803014; K2K WWW page: http://pnahp.kek.jp/.

[26] P. Adamson *et al.* (MINOS Coll.), NuMI-L-476 (March 1999); Web page: http://www.hep.anl.gov/ndk/hypertext/numi.html.

[27] A.G. Cocco *et al.* (OPERA Coll.), Nucl. Phys. Proc. Suppl. **85**, 125 (2000); M. Guler *et al.* (OPERA Coll.), CERN-SPSC-2000-028.

[28] A. Geiser (MONOLITH Coll.), hep-ex/0008067; Web page: http://www.desy.de/~hoepfner/Neutrino/Monolith.

[29] A. Geiser, Talk presented at Neutrino 2000, Sudbury, Canada, 16–21 June 2000 (http://-nu2000.sno.laurentian.ca), hep-ex/0009060.

[30] K. Nakamura (K2K Coll.), Talk presented at Neutrino 2000, Sudbury, Canada, 16–21 June 2000 (http://nu2000.sno.laurentian.ca); M. Sakuda (K2K Coll.), Talk presented at ICHEP2000, Osaka, Japan, July 2000 (http://ichep2000.hep.sci.osaka-u.ac.jp).

[31] G. Mills (LSND Coll.), Talk presented at Neutrino 2000, Sudbury, Canada, 16–21 June 2000 (http://nu2000.sno.laurentian.ca).

[32] Y. Declais *et al.*, Nucl. Phys. **B434**, 503 (1995).

[33] F. Dydak *et al.*, Phys. Lett. **134B**, 281 (1984).

[34] I. E. Stockdale *et al.*, Phys. Rev. Lett. **52**, 1384 (1984).

[35] L. Borodovsky *et al.*, Phys. Rev. Lett. **68**, 274 (1992).

[36] K. Eitel (KARMEN Coll.), hep-ex/0008002; Web page: http://www-ik1.fzk.de/www/-karmen.

[37] L. Ludovici (CHORUS Coll.), Talk presented at Neutrino 2000, Sudbury, Canada, 16–21 June 2000 (http://nu2000.sno.laurentian.ca); Web page: http://choruswww.cern.ch.

[38] M. Mezzetto (NOMAD Coll.), Talk presented at Neutrino 2000, Sudbury, Canada, 16–21 June 2000 (http://nu2000.sno.laurentian.ca); Web page: http://nomadinfo.cern.ch.

[39] A. Bazarko (MiniBooNE Coll.), Talk presented at Neutrino 2000, Sudbury, Canada, 16–21 June 2000 (http://nu2000.sno.laurentian.ca), hep-ex/0009056; Booster Neutrino Experiment (BooNE): http://nu1.lampf.lanl.gov/BooNE.

[40] C. Giunti, hep-ph/9909395.

[41] G.L. Fogli *et al.*, hep-ph/9906450.

[42] S.M. Bilenky, C. Giunti and W. Grimus, Eur. Phys. J. C **1**, 247 (1998), hep-ph/9607372; Proc. of *Neutrino '96*, Helsinki, June 1996, edited by K. Enqvist *et al.*, p. 174, World Scientific, 1997, hep-ph/9609343.

[43] V. Barger, S. Pakvasa, T. J. Weiler, and K. Whisnant, Phys. Rev. **D58**, 093016 (1998), hep-ph/9806328.

[44] S. M. Bilenky, C. Giunti, W. Grimus, and T. Schwetz, Phys. Rev. **D60**, 073007 (1999), hep-ph/9903454.

[45] D. Dooling, C. Giunti, K. Kang, and C. W. Kim, Phys. Rev. **D61**, 073011 (2000), hep-ph/9908513.

[46] C. Giunti, M. C. Gonzalez-Garcia, and C. Pena-Garay, Phys. Rev. **D62**, 013005 (2000), hep-ph/0001101.

[47] C. Giunti, M.C. Gonzalez-Garcia and C. Pena-Garay, hep-ph/0007154; M.C. Gonzalez-Garcia and C. Pena-Garay, hep-ph/0009041.

[48] O. Yasuda, hep-ph/0006319.

[49] A. Yu. Smirnov, Talk presented at Neutrino 2000, Sudbury, Canada, 16–21 June 2000 (http://nu2000.sno.laurentian.ca), hep-ph/0010097; O. Peres, Talk presented at NOW2000, Otranto, Italy, September 2000 (http://www.ba.infn.it/˜now2000).

[50] G.L. Fogli, E. Lisi, A. Marrone and D. Montanino, hep-ph/0009269 (talk presented by E. Lisi at Neutrino 2000, Sudbury, Canada, 16–21 June 2000, http://nu2000.sno.-laurentian.ca).

[51] G.L. Fogli, E. Lisi and A. Marrone, hep-ph/0009299.

[52] V. Barger, B. Kayser, J. Learned, T. Weiler and K. Whisnant, hep-ph/0008019.

[53] G. L. Fogli, E. Lisi, A. Marrone, and D. Montanino, Phys. Lett. **B425**, 341 (1998),

14

hep-ph/9711421.

[54] S. M. Bilenky and C. Giunti, Phys. Lett. **B444**, 379 (1998), hep-ph/9802201.

[55] G. L. Fogli, E. Lisi, D. Montanino, and A. Palazzo, Phys. Rev. **D62**, 013002 (2000), hep-ph/9912231.

[56] Leslie Camilleri (NOMAD Coll.), "NOMAD, A Status Report" Status Report to the SPSC , 14 september 1999 (http://nomadinfo.cern.ch/Public/PUBLICATIONS/-public_pub.html).

[57] L. Mikaelyan, hep-ex/0008063; hep-ex/0008046; Nucl. Phys. Proc. Suppl. **87**, 284 (2000), hep-ex/9910042; L.A. Mikaelyan and V.V. Sinev, hep-ex/9908047.

[58] S. Geer, Phys. Rev. D **57**, 6989 (1998), Erratum *ibid.* D **59**, 039903 (1999), hep-ph/9712290; A. Blondel *et al.*, "The neutrino factory : beam and experiment", CERN-EP-2000-053; C. Albright *et al.*, "Physics at a Neutrino Factory", Report to the Fermilab Directorate, hep-ex/0008064.

[59] N. Fornengo, M. C. Gonzalez-Garcia, and J. W. F. Valle, Nucl. Phys. **B580**, 58 (2000), hep-ph/0002147.

[60] R. Foot, hep-ph/0007065.

[61] D. Dooling, C. Giunti, K. Kang and C.W. Kim, in preparation.

[62] H. Nunokawa, J.T. Peltoniemi, A. Rossi and J.W.F. Valle, Phys. Rev. D **56**, 1704 (1997), hep-ph/9702372; H. Athar and J.T. Peltoniemi, Phys. Rev. D **51**, 5785 (1995).

[63] D.O. Caldwell, G.M. Fuller, Y.Z. Qian, Phys. Rev. D **61**, 123005 (2000), astro-ph/9910175. G.C. McLaughlin, J.M. Fetter, A.B. Balantekin, G.M. Fuller. Phys. Rev. C **59**, 2873 (1999), astro-ph/9902106.

[64] R.R. Volkas, hep-ph/0009162; P. Di Bari, R. Foot, R.R. Volkas and Y.Y.Y. Wong, hep-ph/0008245; P. Di Bari and R. Foot, hep-ph/0008258.

[65] D.P. Kirilova and M.V. Chizhov, hep-ph/9909408; hep-ph/9908525; Nucl. Phys. B **534**, 447 (1998), hep-ph/9806441.

[66] A.D. Dolgov, S.H. Hansen, S. Pastor, D.V. Semikoz, Astropart. Phys. **14**, 79 (2000), hep-ph/9910444.

[67] S. Esposito, G. Mangano, A. Melchiorri, G. Miele and O. Pisanti, astro-ph/0007419.

[68] X. Shi and G.M. Fuller, Phys. Rev. D **59**, 063006 (1999), astro-ph/9810075; astro-ph/9812232; K. Abazajian, X. Shi and G.M. Fuller, astro-ph/9904052; astro-ph/-9905259.

[69] S.P. Mikheyev and A.Yu. Smirnov, Yad. Fiz. **42**, 1441 (1985) [Sov. J. Nucl. Phys. **42**, 913 (1985)]; Il Nuovo Cim. C **9**, 17 (1986); L. Wolfenstein, Phys. Rev. D **17**, 2369 (1978); Phys. Rev. D **20**, 2634 (1979).
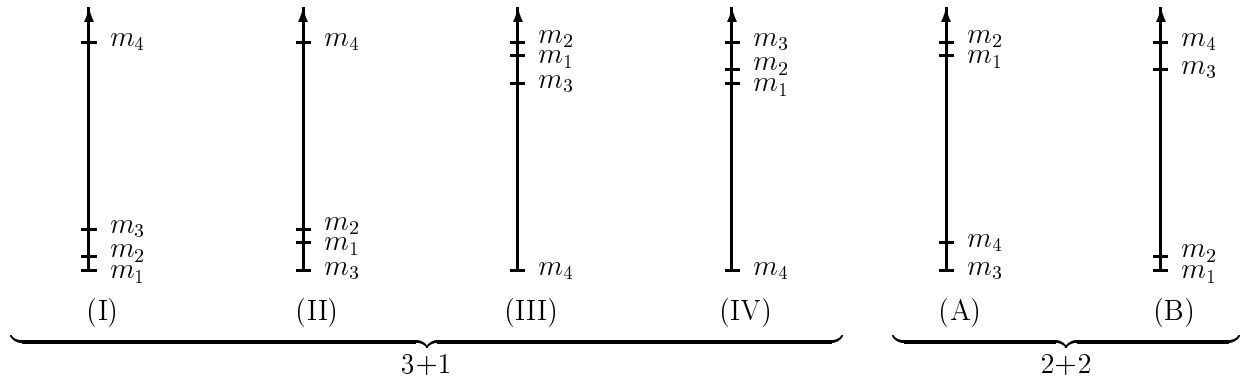
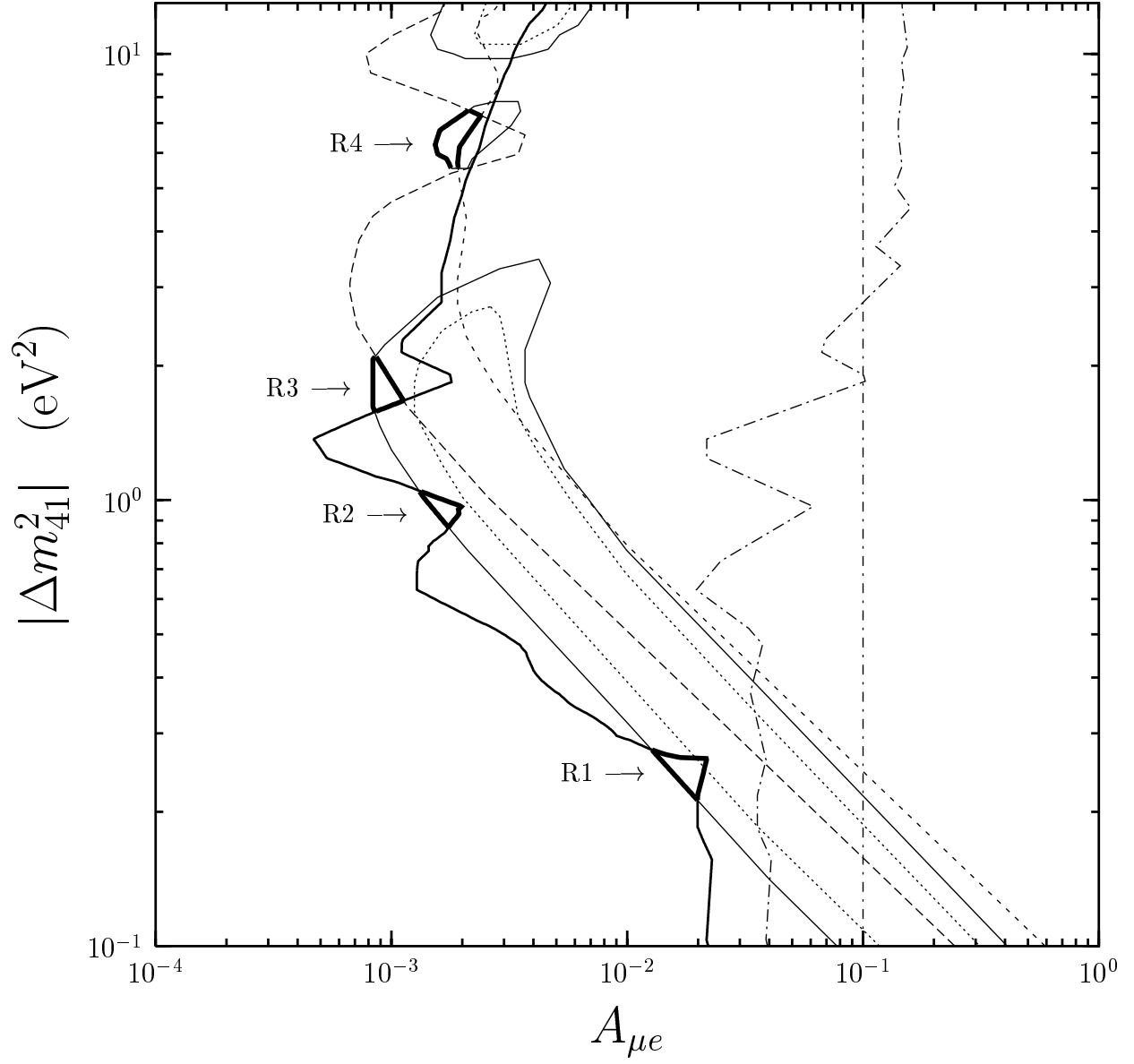FIG. 1.   Qualitative illustration of the possible four-neutrino schemes.

FIG. 2. **Very Thick Solid Line:** Allowed regions. **Thick Solid Line:** Disappearance bound (3.5). **Dotted Line:** LSND 2000 allowed regions at 90% CL [31]. **Solid Line:** LSND 2000 allowed regions at 99% CL [31]. **Broken Dash-Dotted Line:** Bugey exclusion curve at 90% CL [32]. **Vertical Dash-Dotted Line:** CHOOZ exclusion curve at 90% CL [23]. **Long-Dashed Line:** KARMEN 2000 exclusion curve at 90% CL [36]. **Short-Dashed Line:** BNL-E776 exclusion curve at 90% CL [35].
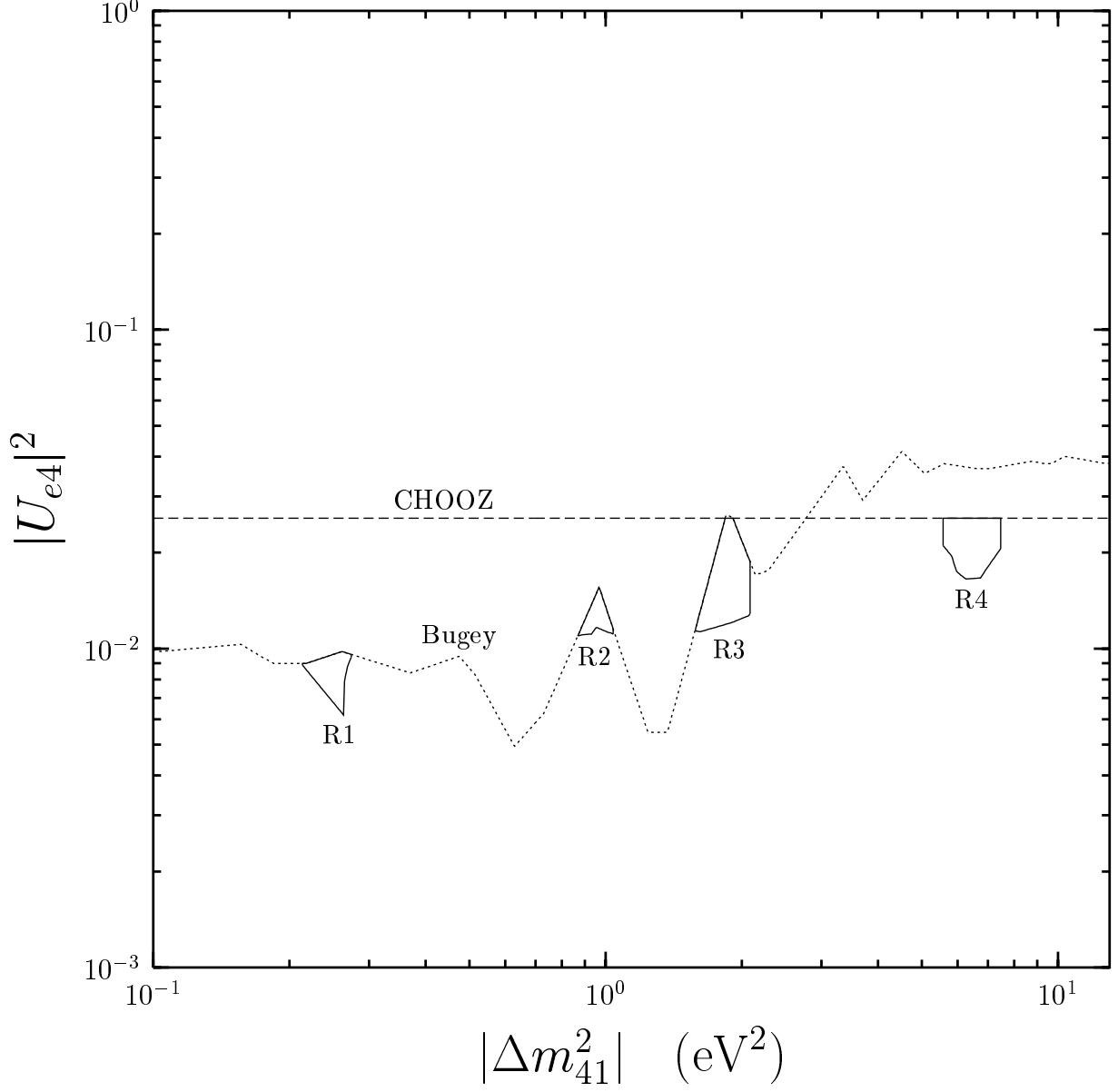
FIG. 3.   **Dotted Line:** $|U_{e4}|^2_{\max}$ obtained from the 90% CL exclusion curve of the Bugey short-baseline reactor $\bar{\nu}_e$ disappearance experiment [32] (Eq. (3.2)). **Dashed Line:** $|U_{e4}|^2_{\max}$ obtained from the 90% CL exclusion curve of the CHOOZ long-baseline reactor $\bar{\nu}_e$ disappearance experiment [23] (Eq. (3.2)). **Solid Line:** Allowed regions (Eq. (3.9)).
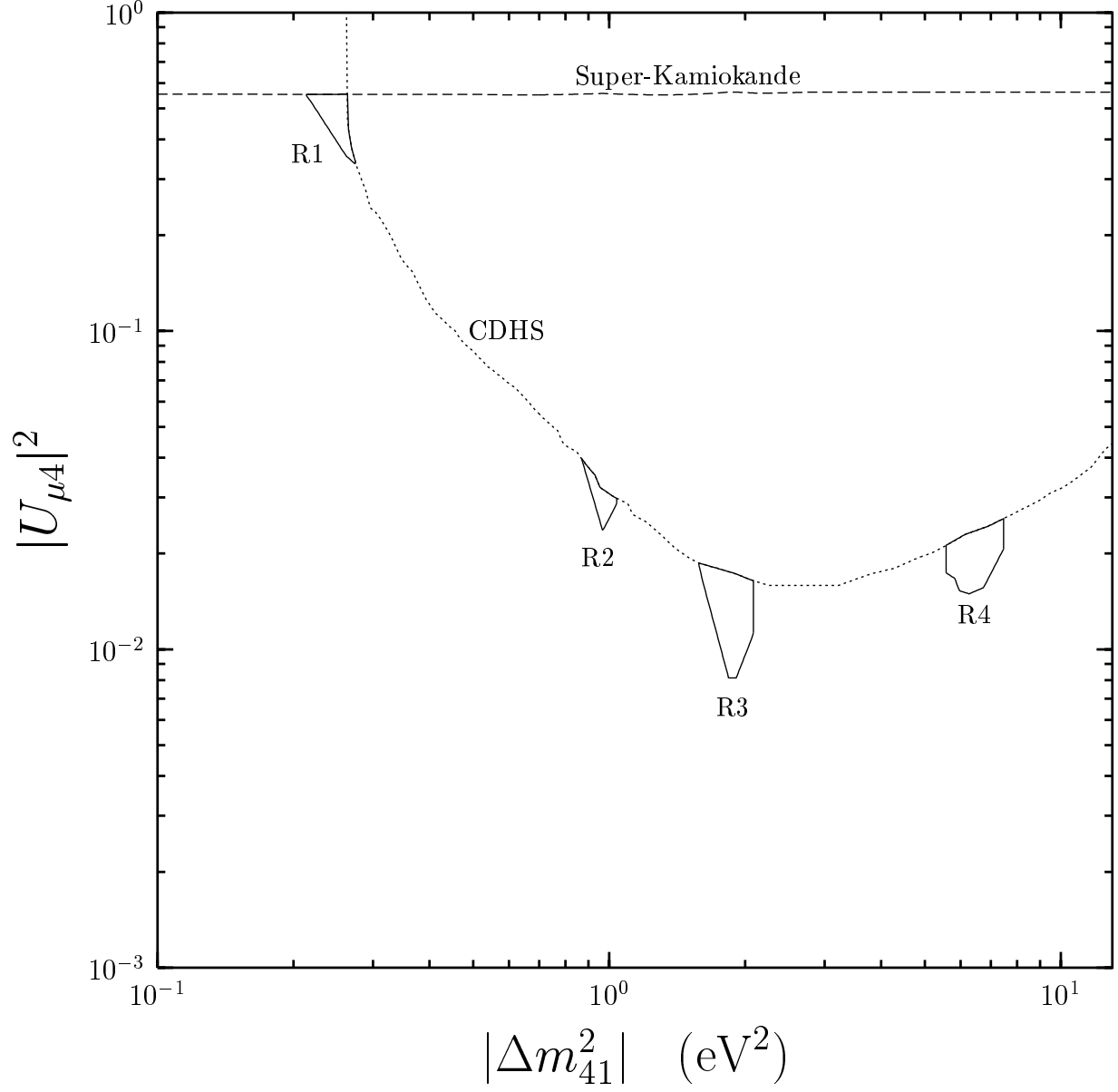
FIG. 4. **Dotted Line:** $|U_{\mu 4}|^2_{\max}$ obtained from the exclusion curve of the CDHS accelerator ν_μ disappearance experiment [33] (Eq. (3.3)). **Dashed Line:** $|U_{\mu 4}|^2_{\max}$ obtained from the up-down asymmetry of multi-GeV muon-like events measured in the Super-Kamiokande experiment [20] (Eq. (3.3)). **Solid Line:** Allowed regions (Eq. (3.10)).
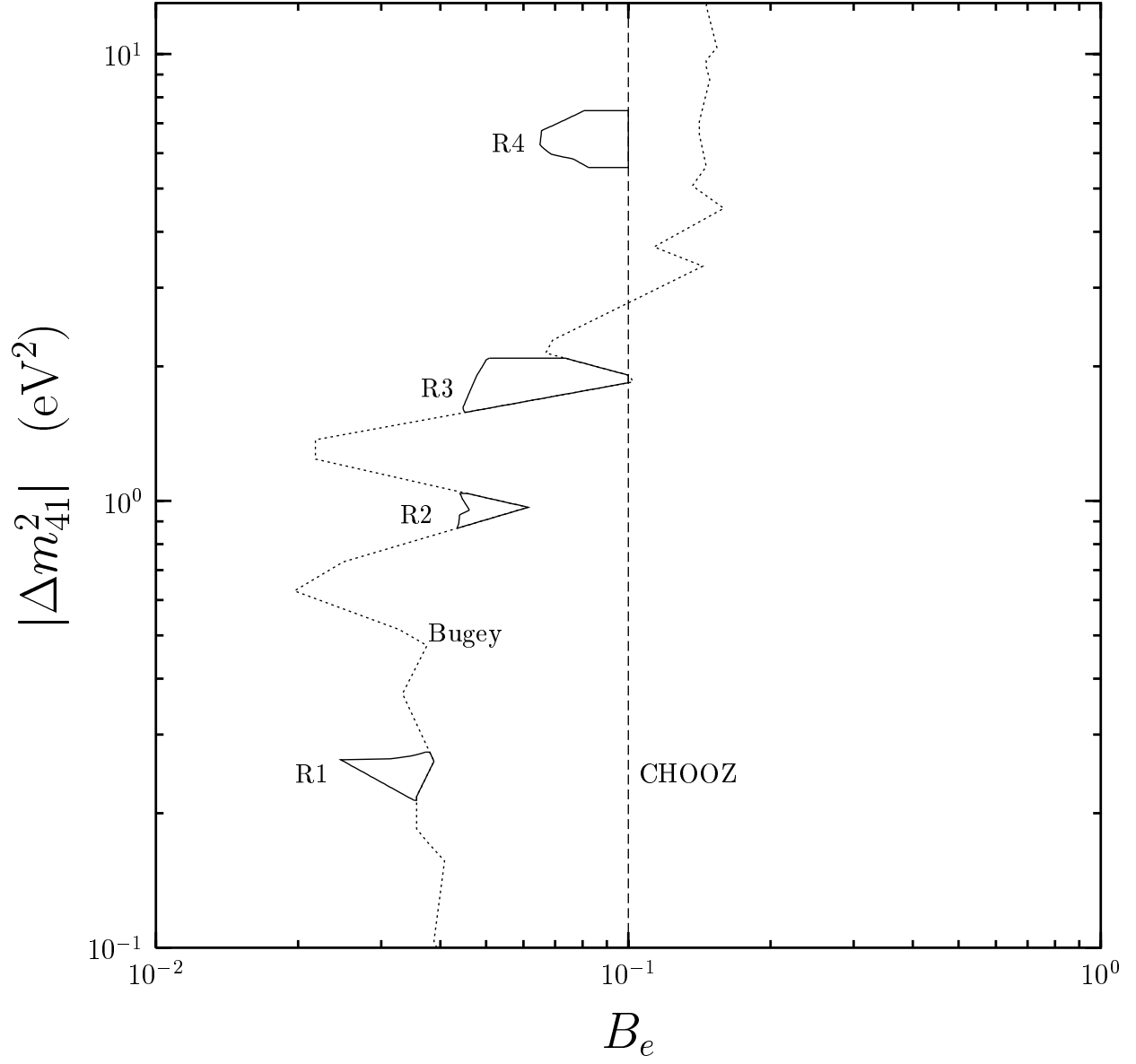
FIG. 5. **Solid Line:** Allowed regions. **Dotted Line:** Bugey exclusion curve at 90% CL [32]. **Dashed Line:** CHOOZ exclusion curve at 90% CL [23].
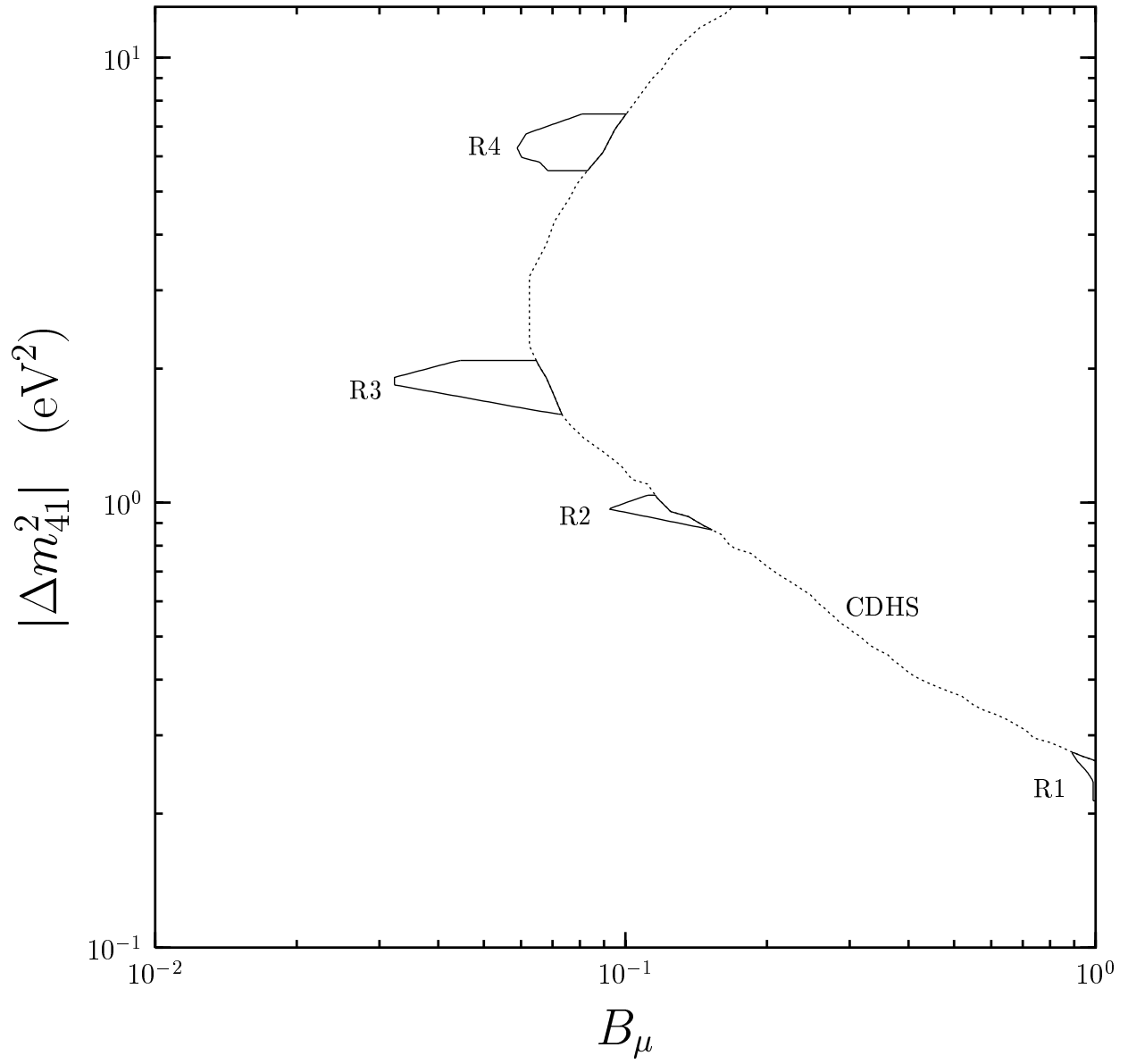
FIG. 6. **Solid Line:** Allowed regions. **Dotted Line:** CDHS exclusion curve at 90% CL [33].
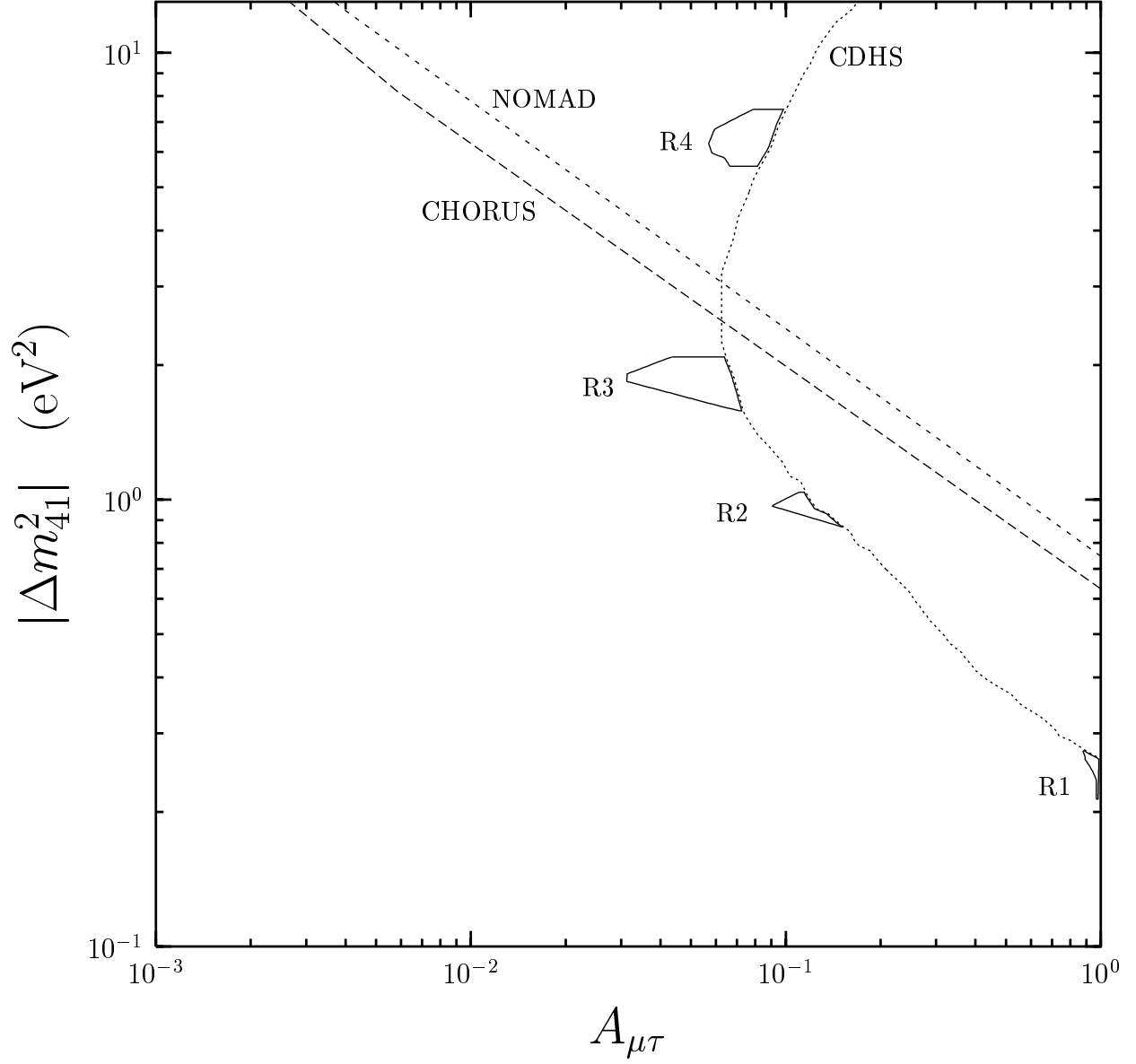
FIG. 7. **Solid Line:** Allowed regions. **Long Dashed Line:** CHORUS exclusion curve at 90% CL [37]. **Short Dashed Line:** NOMAD exclusion curve at 90% CL [38]. **Dotted Line:** CDHS exclusion curve at 90% CL [33].
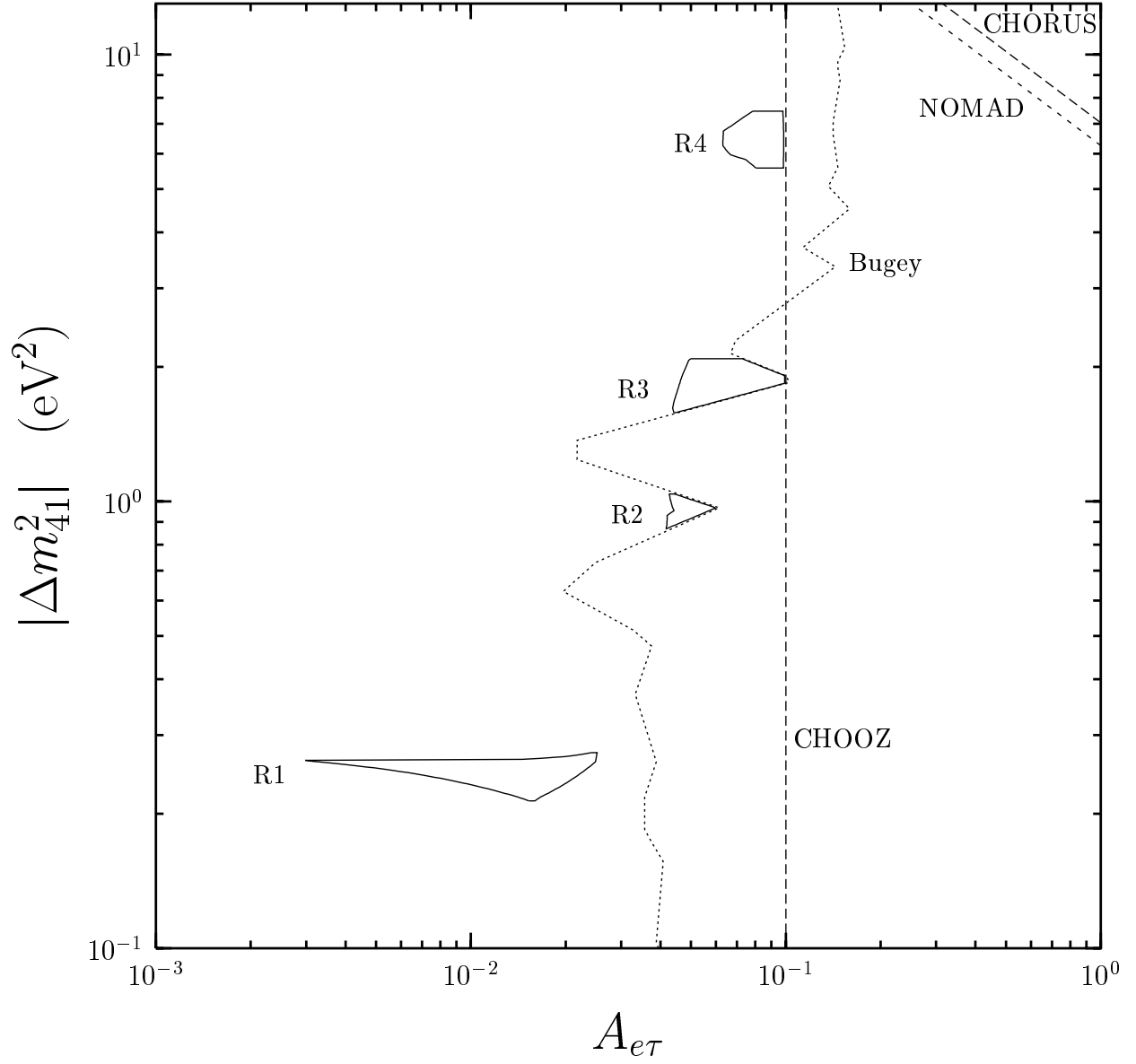
FIG. 8. **Solid Line:** Allowed regions. **Long Dashed Line:** CHORUS exclusion curve at 90% CL [37]. **Short Dashed Line:** NOMAD exclusion curve at 90% CL [38]. **Dotted Line:** Bugey exclusion curve at 90% CL [32]. **Dashed Line:** CHOOZ exclusion curve at 90% CL [23].